Acta Geotechnica (2021) 16:3947–3961
https://doi.org/10.1007/s11440-021-01363-x

RESEARCH PAPER

The impact of stress disturbance on undrained cyclic behaviour of a kaolin clay and settlement of tunnels under cyclic loading

Zhiyong Liu[1,2] · Jianfeng Xue[1] · Guoxiong Mei[2]

Received: 23 April 2021 / Accepted: 17 September 2021 / Published online: 6 October 2021

Abstract
The excavation of a pit or tunnel induces stress disturbances in soils under different stress paths. The cyclic deformation behaviour of soft clay would be affected by the induced stress disturbances. A series of undrained cyclic triaxial tests were performed on a normally consolidated kaolin clay. The stress disturbance was simulated by changing the radial and axial stresses between loading cycles under different stress paths. The effects of stress disturbance schemes on the axial strain and excess pore water pressure accumulation in the clay were presented and discussed. The results indicate that for the samples experiencing stress disturbance with no change in static deviatoric stress, during the subsequent bundle of loading cycles, the axial strain and excess pore water pressure accumulate slightly in the early few cycles and then roughly follow the accumulation tendency similar to that of the sample under continuous cyclic loading. If the static deviatoric stress reduces, after including stress disturbance, axial strain and excess pore water pressure accumulate slightly in the early few cycles and keep almost constant afterwards, regardless of stress disturbance schemes. The accumulation rates of axial strain and excess pore water pressure during the subsequent loading cycles increase if positive static deviatoric stress is induced, and the greater the induced additional static deviatoric stress, the greater the strain accumulation. The axial strain accumulation is governed by static deviatoric stress ratio (q/p'), and independent to stress disturbance schemes. Based on the variation of axial strain accumulation under different stress disturbance schemes, two examples are presented to explain the impact of nearby excavations to the long-term deformation of existing tunnels under cyclic loading.

Keywords Cyclic triaxial tests · Long-term settlement of tunnels · Soft clay · Stress disturbance

1 Introduction

Big cities in coastal areas are under the pressure of traffic congestion. More and more pits and tunnels will be inevitably constructed nearby existing roads, railways and tunnels which are subjected to long-term repeated loading. The construction activities will change the stress states in soils along different stress paths and affect the cyclic deformation behaviour of soils, especially soft clays. Understanding the cyclic deformation behaviour of soft clay with stress disturbances between loading cycles is critical for estimating repeated loading-induced long-term settlement of existing structures adjacent to new excavations.

Large unexpected long-term settlement of roads or tunnels in soft clay has been observed after opening to traffic [3, 25, 33, 35]. Previous studies have illustrated that traffic loading is one of the reasons for the large settlement [2, 6, 21, 22]. For example, Chai and Miura [3] analysed the long-term settlement of Saga Airport Road in highly compressible Ariake clay. The author sclaimed that the traffic loading-induced settlement can reach about 225 mm within four years after opening to traffic. Ren et al. [24] reported that the settlement of Shanghai metro line 1 developed about 60 mm during the first 8 months of operation in 1995, but very limited settlement was observed before that. Ge et al. [9] investigated the settlement of Shanghai metro line 9 and claimed that the traffic

✉ Jianfeng Xue
jianfeng.xue@adfa.edu.au

[1] School of Engineering and Information Technology, University of New South Wales, Campbell, ACT 2612, Australia

[2] Guangxi Key Laboratory of Disaster Prevention and Engineering Safety, Guangxi University, Nanning, China

loading-induced settlement would be over two-thirds of the total post-construction settlement. Yang and Cui [34] evaluated the traffic loading-induced settlement of a railway in soft clay and reported that under the train speed of about 400 km/h, the settlement developed in the track is about 35 mm within 10,000 train passes.

To evaluate the long-term settlement of road or tunnel subjected to repeated loading, cyclic tests are normally required to determine the deformation behaviour of soft clays. It has been well recognised that the undrained cyclic deformation characteristics of soils highly depend on the stress state and the amplitude of cyclic stress [2, 12, 15, 21, 30, 31]. Qian et al. [23] performed a series of undrained cyclic tests on Shanghai clay under various effective mean consolidation stresses and cyclic stress ratios (the ratio of cyclic stress to effective mean consolidation stress). The authors claimed that the undrained strain accumulation can be described using shakedown theory. For soils subjected to small cyclic stress ratio, axial strain accumulation is attributed to the adjustment in microstructure, and increment of plastic strain per each cycle tends to be negligible as loading cycles continue. Yang and Cui [34] studied the cyclic deformation behaviour of soft clay under intermittent cyclic loading and found that the accumulated plastic strain increases exponentially with the increase of cyclic stress ratio. Hyodo et al. [14] and Chen et al. [4] claimed that applying greater static deviatoric stress results in greater axial strain accumulation as the stress state in the sample gets closer to the failure envelope of the soil. To consider the effects of stress rotation in traffic loading on the deformation behaviour of soft clay, Wang et al. [31] carried out a series of cyclic torsional shearing tests on Wenzhou clay using a hollow cylinder apparatus. The authors reported that the stress–strain curves of the clay are governed by the amplitude of cyclic stress and initial confining pressure. The finding was supported by Qian et al. [23] with a series of cyclic torsional shearing tests on Shanghai clay.

As suggested by Shen et al. [25] and Ou et al. [18], in addition to cyclic loading, the disturbance from nearby construction is also a possible reason for such unexpected greater settlement of metro tunnels or railways. This is because the construction activities change the stress states in soils under different stress paths [10, 17, 26–28, 36] and affect the cyclic deformation characteristics of soils within the influenced zones. This means that the effects of including various stress disturbances between loading cycles should be considered in analysing the soil's deformation behaviour under subsequent cyclic loadings.

For existing studies on cyclic tests, however, the cell pressure and initial static deviatoric stresses were kept unchanged during cyclic loading process; therefore, the stress disturbance-induced soil deformation under cyclic loading has not been considered. There are very limited studies on the effects of including stress disturbance between loading cycles on the long-term deformation behaviour of soft clay. Liu et al. [16] considered the effects of unloading lateral stress between loading cycles on the deformation of a kaolin clay. The authors reported that including lateral unloading increases the strain accumulation and the greater the reduction in lateral stress, the greater the strain accumulation during the subsequent loading cycles. However, the work is limited to lateral unloading, whilst the stress state in soil may be disturbed in different stress paths, i.e. the static deviatoric stress would decrease, increase or remain unchanged during stress disturbance. The effects of stress disturbance under different stress paths on the deformation behaviour of soft clay under cyclic loading need to be further investigated.

To identify the effects of including various stress disturbances between loading cycles on the long-term deformation behaviour of soft clay, this paper reports the results of a series of undrained cyclic triaxial tests on a normally consolidated kaolin clay. The stress disturbance is simulated by changing radial and axial stresses with different magnitudes between loading cycles. The axial strain and excess pore water pressure (EPWP) accumulations are presented and discussed under different stress disturbance schemes, to consider the effects of decreasing, increasing or maintaining static deviatoric stress between loading cycles. The results are used to demonstrate the possible impact of the excavation of a new pit or tunnel on traffic loading-induced settlement of existing tunnels considering the relative locations of the existing tunnels to the new projects.

2 Sample preparation and test program

2.1 Sample preparation

The material used in the test is a kaolin clay with a specific gravity of 2.6. The plastic limit and liquid limit are about 35% and 75%, respectively, with a plasticity index (*PI*) of about 40%. Kaolin slurry with the water content of about two times of liquid limit was put into a Perspex tube with an internal diameter of 50 mm to prepare cylindrical samples. After being one-dimensionally consolidated under the vertical surcharge of about 100 kPa, the samples were extruded from the tube. The heights of the samples range from 59 to 71 mm. According to Wichtmann et al. [32], the dimensions of samples would have limited effects on the response of clay under cyclic triaxial loading. Samples of different heights have also been used by Jamali et al. [15], therefore the samples were not trimmed to the same height after pre-consolidation. The samples were then saturated in

the triaxial cell under a back pressure of 300 kPa and effective confining pressure of 20 kPa to reach a Skempton's B value of at least 0.98. The samples were isotropically consolidated under the effective confining pressure of 100 kPa, followed by anisotropic consolidation to the deviatoric stress of 25 kPa. As recommended by Liu et al. [16], a few pieces of filter paper strips were put along the sides of samples to accelerate the saturation and consolidation process. Consolidation duration was kept long enough to allow the full dissipation of excess pore water pressures in all samples. In addition, possible creep was allowed in samples. The axial strain at the end of consolidation is 0.006–0.013% per hour (except DD2 which is with the strain rate of 0.018% per hour due to less consolidation duration). This means that all samples have completed primary consolidation and have similar consolidation results.

2.2 Test program

The tests were performed using an advanced Dynamic Triaxial Testing System manufactured by GDS Instruments Ltd., UK. This system is capable of performing both axial force and displacement-controlled cyclic loading tests, with the frequency up to 5 Hz. More details about this system can be found in the work of Qian et al. [21].

After being consolidated, the samples were subjected to 5000 sinusoidal loading cycles under the loading frequency of 0.5 Hz and peak—peak amplitude of 20 kPa. In general, frequency has limited effects on the cyclic behaviour of soft clay under undrained condition [13, 23]. According to Yang et al. [35], the traffic loading frequency of Shanghai metro ranges from 0.2 to 3 Hz when train speed increases from 20 to 80 km/h. The loading frequency of 0.5 Hz used in this study falls in the above range. Yang et al. [35] calculated Shanghai metro traffic loading in soils at about 11.5 m blow ground surface and found that the vertical cyclic stress is about 14 kPa and shear stress is about 4.5 kPa. Considering in triaxial cell the difficulty in simulating stress rotation which could enlarge strain accumulation [23], the vertical cyclic stress of 20 kPa is adopted, which is greater than the value calculated by Yang et al. [35]. This results in a cyclic stress ratio (the amplitude of cyclic stress to effective mean stress) of about 0.18, which falls in the range of 0.07 to 0.4 as used by Qian et al. [23] in investigating the deformation behaviour of Shanghai clay subjected to traffic loading. The cyclic loading was applied in axial direction under one-way loading pattern and no tensile stress was induced to the samples. Subsequently, the axial and radial stresses were changed in different stress paths to simulate different stress disturbances caused by construction activities, followed by the second bundle of 5000 loading cycles. Static stress disturbance was achieved by increasing or decreasing axial load and cell pressure. The test schemes are summarised in Table 1, in which the effective mean stress p' and deviatoric stress q are defined as:

$$p' = \frac{\sigma_1^{'} + 2\sigma_3^{'}}{3} \tag{1}$$

and

$$q = \sigma_1^{'} - \sigma_3^{'} \tag{2}$$

where σ_1' and σ_3' are the effective major and minor principal stresses, respectively. In the table, the tests are named based on the change of static deviatoric stress after including stress disturbance. UD, DD and AD refer to no change, increase and decrease in static deviatoric stress, respectively.

As recommended by Liu et al. [16], after including the stress disturbances into the samples, the static deviatoric stresses were held for about 10 min to allow the stabilization of induced EPWP before applying subsequent bundle of loading cycles. Due to the low permeability of kaolin clay, the drainage valves were closed during all loading stages to simulate an undrained condition. Similar undrained condition has been widely adopted in analysing the construction process of pits or tunnels in soft clay [5, 7]. To simulate the long-term drainage process during construction and cyclic loading durations, a coupled drainage and cyclic loading condition should be considered. In this study, however, only undrained condition is considered.

Undrained monotonic triaxial tests were performed on isotropically consolidated samples (q_0 = 0 kPa) under different effective confining pressures to obtain the strength parameters of the kaolin clay. The effective friction angle (ϕ_c) was determined to be about 24.5°, resulting in a slope of about 0.96 for the critical state line (CSL) in the p'-q space.

3 Results and discussion

This section presents and discusses the axial strain and EPWP accumulations in the clay samples subjected to various stress disturbances between loading cycles. Table 2 illustrates the axial strain and EPWP developed in each loading stage. For consistency, the axial strains due to monotonic stress disturbances are excluded from the accumulated strains in all the analyses as recommended by Liu et al. [16].

According to Huang et al. [10] and Verruijt [27], the construction of a pit or tunnel will change the stress states in soils along different stress paths, i.e. the static deviatoric stress would decrease (for the soil directly above or below

Table 1 Undrained cyclic triaxial tests series

ID	σ_1' (kPa)	σ_3' (kPa)	q/p'	$\Delta\sigma_3$ (kPa)	$\Delta\sigma_1$ (kPa)	Δq
UD1	125	100	0.23	–	–	–
UD2	125	100	0.23	− 20	− 20	0
DD1	125	100	0.23	− 10	− 20	− 10
DD2	125	100	0.23	+ 10	− 10	− 20
DD3	125	100	0.23	+ 10	0	− 10
AD1	125	100	0.23	− 15	− 10	5
AD2	125	100	0.23	− 5	0	5
AD3	125	100	0.23	0	+ 5	5
AD4	125	100	0.23	− 30	− 20	10
AD5	125	100	0.23	− 20	− 10	10
AD6	125	100	0.23	+ 10	+ 20	10
AD7	125	100	0.23	− 5	+ 5	10
AD8	125	100	0.23	− 10	0	10
AD9	125	100	0.23	0	10	10
AD10	125	100	0.23	− 5	+ 10	15
AD11	125	100	0.23	− 15	0	15
AD12	125	100	0.23	0	+ 15	15
AD13	125	100	0.23	− 5	+ 15	20

σ_1', σ_3' and the static deviatoric stress ratios (q/p') refer to the stress states in samples before applying any cyclic loading; " − " and " + " denote the decreasing or increasing of stress, respectively; $\Delta\sigma_1$ and $\Delta\sigma_3$ are magnitudes of variation in axial stress (total major principal stress) and radial stress (total minor principal stress), respectively; Δq is the induced additional static deviatoric stress due to the stress disturbance

excavation), increase (for soil next to excavation) or remain unchanged (for soil in some other influenced zone or far away from excavation). Therefore, the tests results are presented in three categories: undisturbed or no induced static deviatoric stress (UD), decreasing static deviatoric stress (DD) and increasing static deviatoric stress (AD) to analyse the possible effects of nearby excavation on the cyclic loading-induced settlement of existing structures. The additional stress induced by the construction of a pit or tunnel will be discussed in more details later.

3.1 Variation of strain and EPWP

3.1.1 No induced static deviatoric stress

Two scenarios were considered in the tests: a sample (UD1) under continuous cyclic loading with no static stress disturbance, and a sample (UD2) with static stress disturbances but with no change in deviatoric stress between loading cycles.

Figure 1a illustrates stress–strain curve in the sample (UD1) without any stress disturbance, i.e. under continuous cyclic loading. The stress–strain curve loops are wide open in the first few cycles and become narrower as loading cycles continue. This suggests that the axial strain accumulation develops sharply in the early few cycles and then tends to increase at a diminishing rate afterwards, which is better shown in Fig. 1b. The similar accumulation tendency is also observed with respect to EPWP. Since no stress disturbance is induced to the sample, the axial strain and EPWP accumulate continuously and steadily during the whole loading period. Figure 1c reveals the effective stress paths in the sample. As loading cycles continue, with the accumulation of EPWP, the effective stress state moves continuously and steadily towards CSL as no stress disturbance is interspersed between loading cycles.

Figure 2a reveals the stress–strain curve of the sample (UD2) with an isotropic unloading of 20 kPa, with no induced static deviatoric stress in the sample during the stress disturbance. As can be seen, the stress–strain hysteretic loop re-opens in the 5001st cycle, suggesting plastic strain accumulation. Such phenomena can be better found in Fig. 2b which illustrates the axial strain and EPWP accumulations in the sample. The axial strain accumulation experiences a slight increase after applying such stress disturbance and then roughly follows the accumulation tendency observed in the sample UD1 as shown in Fig. 1.

Since the stress disturbance is applied under an undrained condition and the sample has a high Skempton's B value (greater than 0.98), as illustrated in Fig. 2b and

Table 2 The axial strain and EPWP developed during each bundle of loading cycles and stress disturbance stage

ID	1 − 5000 cycles			Stress disturbance		After stress disturbance							5001 − 10,000 cycles	
	ε_{1-5000} (%)	$EPWP_1$ (kPa)	q/p'^{a}	ε^S (%)	$EPWP^S$ (kPa)	σ_1 (kPa)	σ_3 (kPa)	σ_1' (kPa)	σ_3' (kPa)	p' (kPa)	q (kPa)	q/p'^{b}	$\varepsilon_{5001-10,000}$ (%)	$EPWP_2$ (kPa)
UD1	0.30	16.1	0.27	–	–	425	300	109.0	84.0	92.3	25.0	0.27	0.032	0.4
UD2	0.31	15.0	0.27	− 0.035	− 19.9	405	280	110.2	85.2	93.5	25.0	0.27	0.036	4.9
DD1	0.26	15.0	0.27	− 0.082	− 16.8	405	290	106.6	92.5	97.2	14.0	0.14	0.02	5.1
DD2	0.33	17.5	0.28	− 0.215	− 2.4	415	310	99.1	93.9	95.6	5.2	0.05	0.01	6.5
DD3	0.27	15.8	0.27	− 0.067	1.5	425	310	108.5	93.2	98.3	15.2	0.16	0.02	4.8
AD1	0.22	13.7	0.26	− 0.006	− 13.4	415	285	114.9	84.7	94.8	30.2	0.32	0.19	6.8
AD2	0.23	14.7	0.27	0.003	− 4.9	425	295	115.1	84.9	95.0	30.2	0.32	0.19	7.2
AD3	0.22	15.2	0.27	0.009	− 0.4	430	300	117.2	86.9	97.0	30.3	0.31	0.19	8.1
AD4	0.26	13.4	0.26	− 0.009	− 24.6	405	270	116.7	81.5	93.2	35.2	0.38	0.89	14.3
AD5	0.29	15.6	0.27	0.007	− 16.2	415	280	114.9	79.8	91.5	35.1	0.38	1.05	16.1
AD6	0.30	16.4	0.27	0.007	9.6	445	310	120.4	85.1	96.9	35.2	0.36	0.59	14.4
AD7	0.24	13.6	0.26	0.018	− 3.3	430	295	120.6	85.3	97.0	35.3	0.36	0.63	14.2
AD8	0.20	14.3	0.27	0.012	− 6.4	425	290	118.7	83.6	95.3	35.1	0.37	0.57	12.3
AD9	0.23	13.3	0.26	0.024	1.3	435	300	121.0	85.6	97.4	35.4	0.36	0.93	17.2
AD10	0.30	15.5	0.27	0.050	− 0.4	435	295	122.5	82.2	95.6	40.2	0.42	1.97	23.9
AD11	0.28	14.4	0.27	0.040	− 9.6	425	285	120.4	80.3	93.6	40.1	0.43	2.71	26.5
AD12	0.23	14.9	0.27	0.039	3.5	440	300	122.2	81.9	95.3	40.2	0.42	1.94	25.0
AD13	0.27	13.8	0.26	0.201	2.3	440	295	125.5	80.4	95.4	45.1	0.47	> 5	> 40

ε_{1-5000} and $\varepsilon_{5001-10,000}$ refer to the axial strains during the first bundle of 5000 cycles (1–5000) and the second bundle of 5000 cycles (5001–10,000), respectively; $EPWP_1$ and $EPWP_2$ are the excess pore water pressures developed during the first bundle of 5000 cycles and the second bundle of 5000 cycles, respectively; ε^S and $EPWP^S$ refer to the axial strain and excess pore water pressure induced by applying stress disturbance; q/p'^{a} and q/p'^{b} correspond to the stress states before including stress disturbance (or after the first bundle of 5000 cycles) and those after including stress disturbance (at the beginning of the 5001st cycle), respectively; σ_1 and σ_3 are total major principal stress (axial stress) and minor principal stress (confining stress), respectively

Table 2, the pore water pressure in the sample decreases by about 19.9 kPa which is almost the same with the reduction of cell pressure (20 kPa). During the subsequent bundle of loading cycles, similar to axial strain accumulation, EPWP develops slightly in the first few cycles and then roughly follows the accumulation tendency in the sample UD1.

The equivalent reduction in pore water pressure means that including isotropic stress disturbance leads no change of stress state in the sample. For example, as indicated in Table 2, the static deviatoric stress ratio (q/p') in the sample UD2 at the beginning of 5001st cycle is about 0.27 which is almost the same with that at the end of the 5000th cycle. This can also be found in Fig. 2c which shows the effective stress paths during cyclic loading stages before and after applying stress disturbance. The stress state is almost unchanged due to applying such stress disturbance. During the subsequent bundle of loading cycles, the stress state in the sample moves steadily towards the CSL, which is similar to that observed in Fig. 1c. Such phenomenon suggests that the slight increase of axial strain accumulation in the early few cycles after including the stress disturbance would not be attributed to the increase of static deviatoric stress ratio in soil. The increment may be because of the soil's ability in memorizing the previous loading history. Due to the application of the stress disturbance, part of the memory in the sample on cyclic behaviour has been erased and the stable state developed in the previous cyclic loading stage is disturbed. Therefore, further cycles are required to reach a new stable state which involves the excess accumulation of strains during the loading cycles after the stress disturbance.

As illustrated in Table 2, the axial strain accumulation developed in the second bundle of 5000 cycles (5001–10,000) in the sample UD2 is about 0.036%, which is similar with that observed in the sample UD1 (0.032%). This means that the axial strain accumulation is hardly affected by stress disturbance if there is no change in static deviatoric stress under undrained condition. Such a phenomenon may suggest that when estimating the long-term settlement of existing structures subjected to cyclic loading, it is acceptable to ignore the stress disturbance if the stress disturbance induces no additional static deviatoric stress in soil.

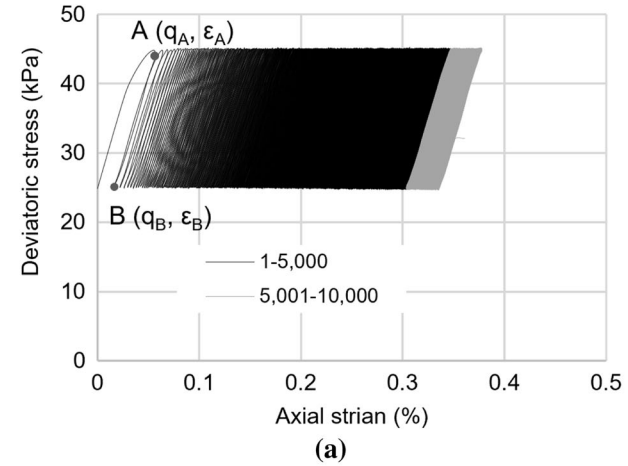

(a)

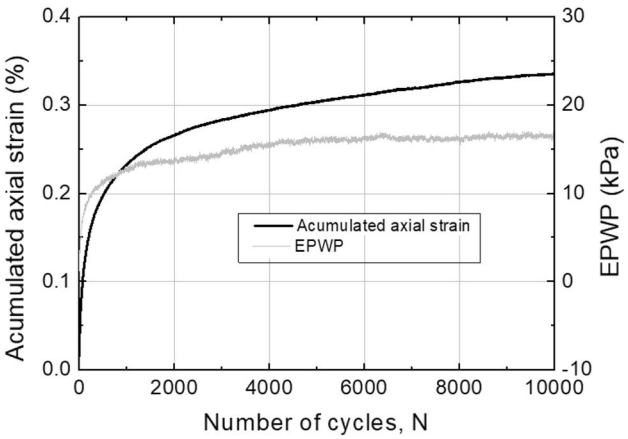

(b)

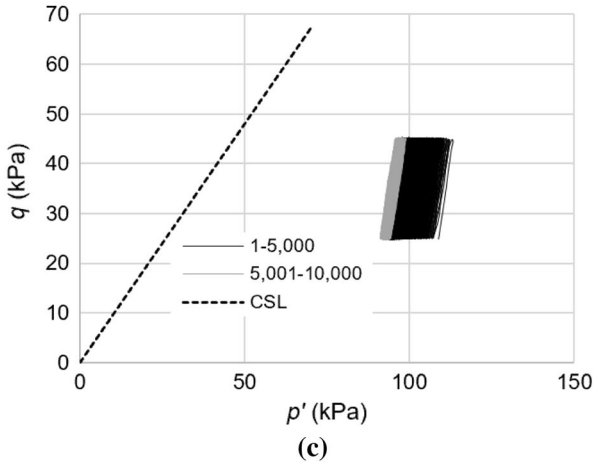

(c)

Fig. 1 **a** The stress–strain curve, **b** the axial strain and EPWP accumulation and **c** effective stress paths in the sample (UD1) under continuous cyclic loading

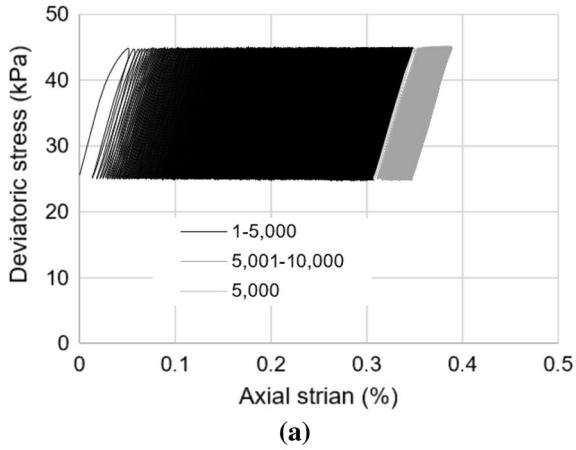

(a)

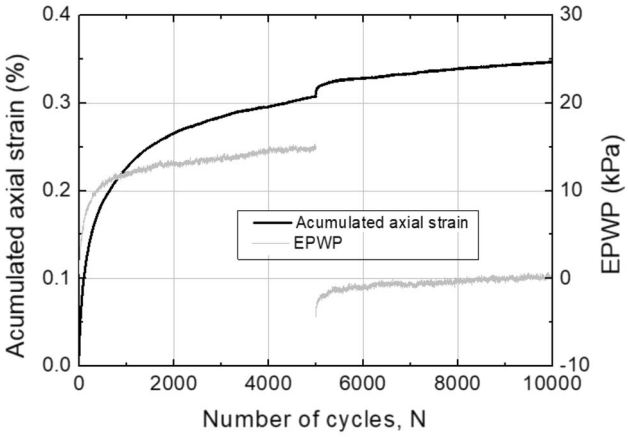

(b)

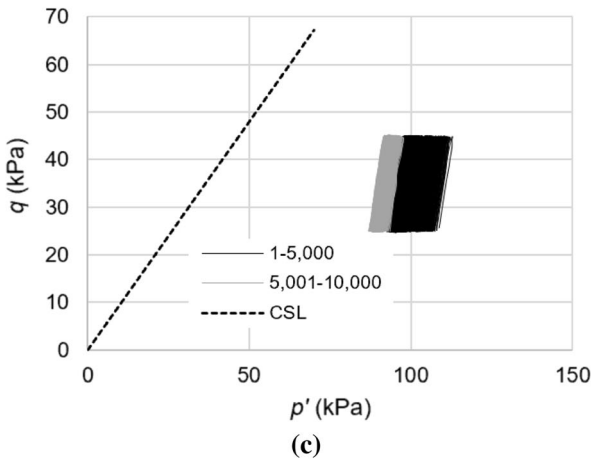

(c)

Fig. 2 **a** The stress–strain curve, **b** the axial strain and EPWP accumulation and **c** effective stress paths in the sample (UD2) experiencing stress disturbance with no change in static deviatoric stress

3.1.2 Decrease static deviatoric stress

Figure 3a illustrates the stress–strain curve observed in the sample (DD1) with the reductions of 20 kPa in major principal stress and 10 kPa in minor principal stress, resulting in the drop of 10 kPa in static deviatoric stress. As can be seen, the stress–strain loop in the sample opens up slightly in the first few cycles after the stress disturbance and closes up quickly afterwards, suggesting that further

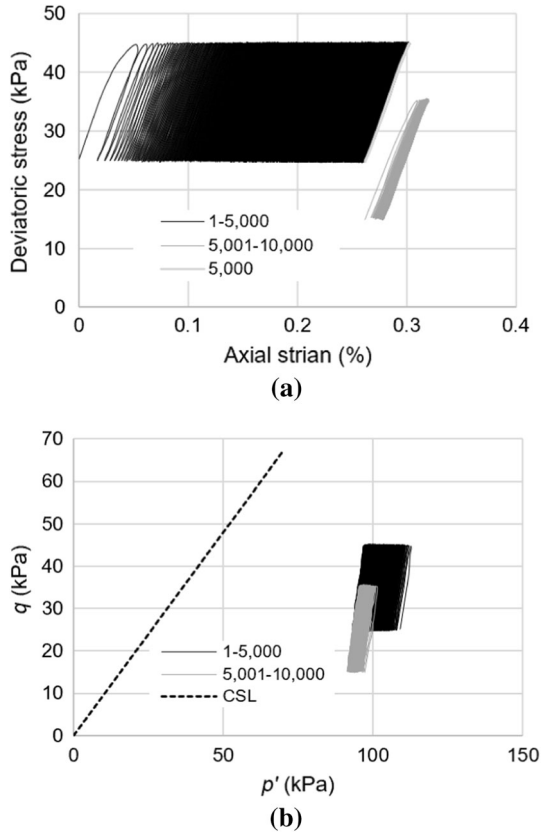

Fig. 3 **a** The stress–strain curve and **b** the effective stress paths in the sample (DD1) subjected to a reduction of static deviatoric stress between loading cycles

loading cycles do not lead to greater accumulation of axial strain. This is better shown in Fig. 4a in which after including the stress disturbance, the axial strain accumulates slightly in the early few cycles and then keeps almost unchanged afterwards, even there is a large drop of EPWP. The reason for such phenomenon can be explained in Fig. 3b which reveals the effective stress paths in the sample. After including such stress disturbance, the stress state moves away from CSL, for example, the static deviatoric stress ratio (q/p') decreases from 0.27 at the end of the 5000th cycle to 0.14 at the beginning of the 5001st cycle. This leads to the reduction of peak deviatoric stress (cyclic stress plus initial deviatoric stress) after applying stress disturbance; therefore, much less strain has been accumulated in the subsequent bundle of loading cycles. Such elimination of axial strain accumulation after a small number of cycles may suggest that compared with that in the samples under continuous cyclic loading, plastic deformation in the samples experiencing static deviatoric stress reduction between loading cycles would be less if loading cycles are large enough.

Figure 4b, c reveals the axial strain and EPWP accumulations in the samples DD2 and DD3, respectively. In the two samples, the lateral stress increased by 10 kPa, and the axial stress in the sample DD2 decreased by about 10 kPa and that in the sample DD3 did not change. This results in the decrements of static deviatoric stress by 20 kPa (sample DD2) and 10 kPa (sample DD3), respectively. The pore water pressures in the samples increase slightly after the stress disturbance as shown in the figures and Table 2. Similar to that in the sample DD1, the axial strains in the two samples increase slightly in the first few cycles and then keep almost constant as cyclic loading continues. This means that as illustrated in Table 2, very limited axial strains accumulate in the samples in the following cyclic loading stage after reducing the static deviatoric stress. The elimination of axial strain accumulation after including such stress disturbance indicates that it may be acceptable to ignore such unloading effect when analysing the repeated loading-induced long-term settlement of existing structures.

3.1.3 Increase static deviatoric stress

Figure 5a illustrates the stress–strain curve of the sample AD7. The sample experienced the reduction of 5 kPa in lateral stress and increase of 5 kPa in axial stress, resulting in the increment of static deviatoric stress by 10 kPa. As can be seen, before including the stress disturbance, the stress–strain curve loop becomes narrower, suggesting that axial strain accumulation rate decreases as cyclic loading continues. After increasing the static deviatoric stress, however, the stress–strain curve loops open up greatly and are even greater than the size of the loop in the first loading cycle. The plastic axial strain developed in the 5001st cycle is about 0.017%, and it is about 0.012% during the 1st cycle, as shown in Fig. 6a. This suggests that the axial strain accumulation in the sample is enlarged due to the stress disturbance. This is because as illustrated in Fig. 5b, the stress state gets closer to CSL after including such stress disturbance, for example, the static deviatoric stress ratio (q/p') increases from 0.26 at the end of the 5000th cycle to 0.36 at the beginning of 5001st cycle, which is also shown in Table 2.

Figure 6 also illustrates the axial strain and EPWP accumulations of two other samples (AD11 and AD14)) that have been subjected to the same reduction (5 kPa) in lateral stress but different increases in axial stress: 10 kPa in AD11 and 15 kPa in AD14. This results in the increases in static deviatoric stress by 15 kPa in AD11 and 20 kPa in AD 14, respectively, as shown in Table 2. The figure and the table suggest that the greater the induced additional static deviatoric stress (Δq), the greater the axial strain and EPWP accumulations in the subsequent bundle of loading cycles. For example, the axial strain accumulations during the subsequent 5000 cycles are about 0.63% (sample AD7,

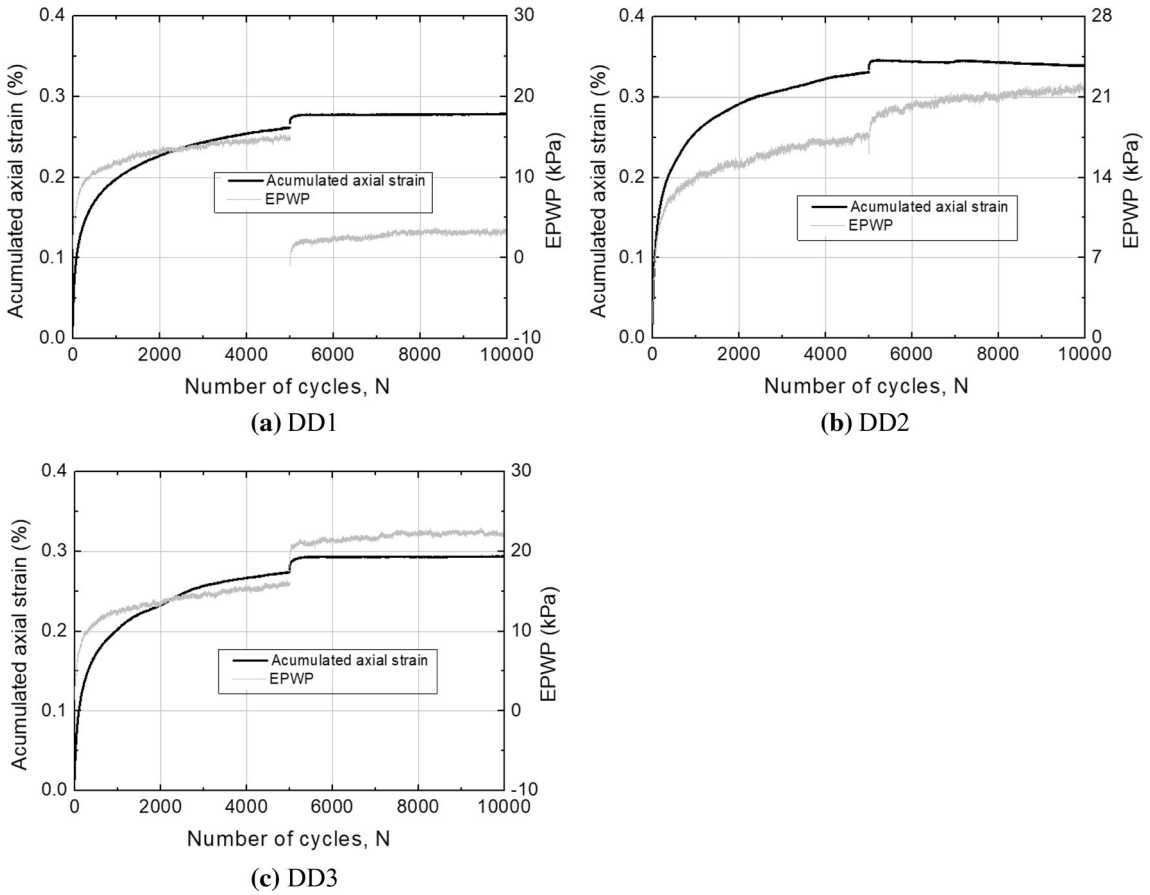

Fig. 4 The axial strain and EPWP accumulations in samples subjected to different amplitude of reduction in static deviatoric stress between loading cycles

Δq = 10 kPa) and 1.97% (sample AD11, Δq = 15 kPa), respectively. For the sample (AD14) with the increment of 15 kPa in axial stress (Δq = 20 kPa), the axial strain increases sharply with loading cycles and the sample fails within 573 loading cycles. Similar trend in EPWP accumulation can also be observed in Fig. 6b and Table 2. The increments of axial strain and EPWP accumulations under the subsequent bundle of loading cycles suggest that, if static deviatoric stress is anticipated to increase, then its effect should be considered in analysing the deformation of ground under cyclic loading condition.

Similarly, under other schemes of stress disturbance, as revealed in Table 2, the axial stain and EPWP accumulations increase with the induced additional static deviatoric stresses (Δq). The greater the Δq, the greater is the increment. This can be better found in Fig. 7a which illustrates the axial strain accumulations developed in the second bundle of 5000 cycles (5001–10,000) in the samples with static deviatoric stress increasing. The axial strains are normalized by those developed in the first bundle of 5000 cycles (1–5000). As can be seen, under various stress disturbances, axial strain accumulates almost exponentially with the induced additional static deviatoric stress.

Figure 7a also shows that, the normalized axial strains developed in the second bundle of 5000 cycles (5001–10,00) could be different even under the same induced additional static deviatoric stress level (particularly at great Δq conditions) and have no clear relationship with stress disturbance schemes. For example, under Δq = 10 kPa, the normalized strain varies between 2 and 4 for different samples. This is because as revealed in Table 2, even at the same Δq condition, the effective mean stress (p') is slightly different. This leads to the slight variation of the static deviatoric stress ratio (q/p') at the beginning of the 5001st cycle even under the same Δq condition. According to Chen et al. [4], under continuous cyclic loading, axial strain and EPWP accumulation increases with static deviatoric stress ratio as the stress state gets closer to the failure envelope of the soil.

Figure 7b shows the dependence of normalized axial strain accumulation on static deviatoric stress ratio. It is to note that, in the figure, all the samples were under almost the same stress state (q/p' = 0.26–0.27) before applying

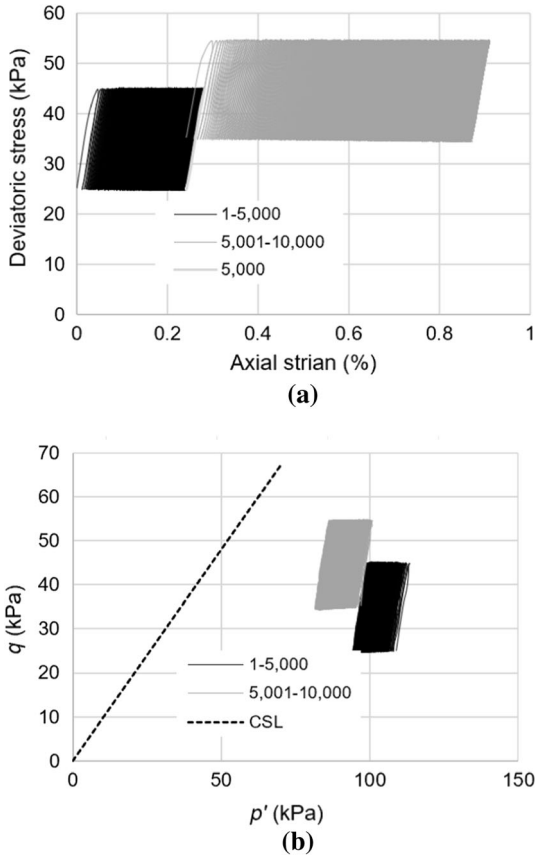

Fig. 5 **a** The stress–strain curve and **b** effective stress paths in a sample (AD7) subjected to an increase of static deviatoric stress between loading cycles

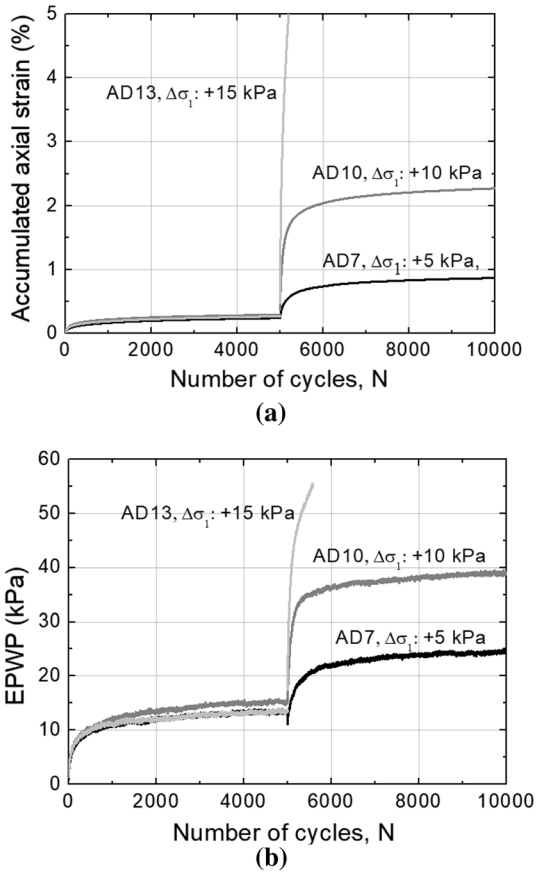

Fig. 6 The axial strain (**a**) and EPWP (**b**) accumulation in the samples subjected to different levels of increment in static deviatoric stress (under lateral unloading of 5 kPa)

stress disturbance as shown in Table 2. As can be seen, the strain accumulations developed in the subsequent cycles have a near exponential relationship with the static deviatoric stress ratio (q/p'), regardless of the stress disturbance schemes. Such exponential relationship suggests that under the same increment of static deviatoric stress, small variation in p' value induced by any other disturbance, such as EPWP, could lead to notable variation in axial strain developed in the subsequent cycles as seen in Fig. 7a. In addition, the exponential relationship supports the claims by Liu et al. [16] that, the enlargement of axial strain and EPWP accumulation after including stress disturbance between loading cycles is attributed to the increase of static deviatoric stress ratio (q/p') and soil's ability in memorizing the previous loading history, as the soil's ability in memorizing the previous loading history increases with the increase of static deviatoric stress.

The reason why the stress disturbance schemes have little effect on the relationship between the strain accumulation and the static deviatoric stress ratio is that, under undrained condition, for fully saturated samples, changing cell pressure (isotropic loading or unloading) will not affect effective stress in the samples. Therefore, the effects of stress disturbances on the stress states of the samples would be only attributed to the change of static deviatoric stress ratio (q/p'). So, similar axial strain accumulation would be expected under the same variation of static deviatoric stress ratio, regardless of the schemes of stress disturbance.

3.2 Variation of resilient modulus

The resilient modulus (Mr) can be calculated using:

$$Mr = \frac{q_A - q_B}{\varepsilon_A - \varepsilon_B} \tag{3}$$

where q_A is approximate 90% of maximum deviatoric stress and q_B refers to minimum deviatoric stresses in an unloading cycle as shown in Fig. 1a; ε_A and ε_B refer to the axial strains at q_A and q_B in an unloading cycle, respectively. As suggested by Alam et al. [1], the selection of approximate 90% of maximum deviatoric stress is to ensure the consistency of data.

The evolution of resilient modulus in the sample UD1 is illustrated in Fig. 8a where the stiffness degrades during the first few cycles, and then increases slightly. The

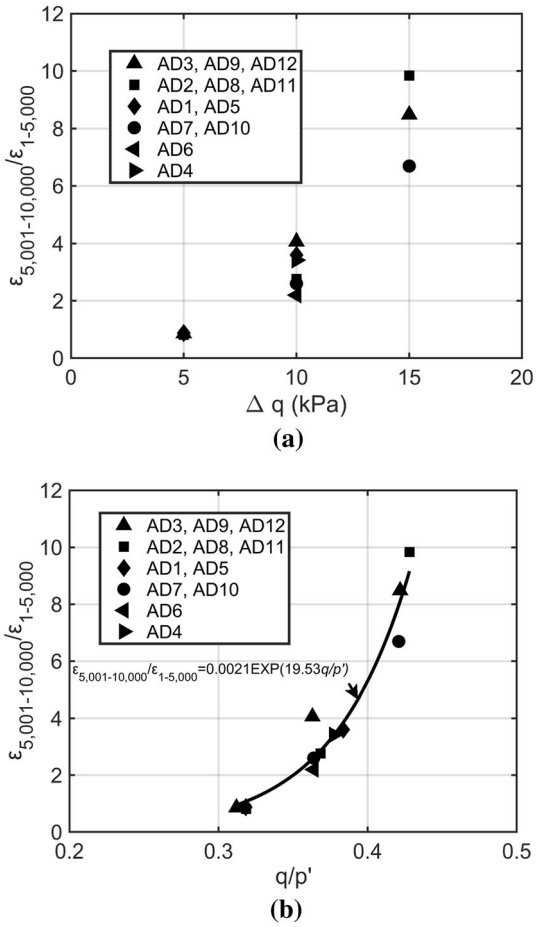

Fig. 7 The relationship of normalized axial strain accumulations with **a** induced additional static deviatoric stress (Δq) and **b** static deviatoric stress ratio (q/p')

increase of stiffness in soils under undrained cyclic loading was also reported by Qian et al. [19, 20] and Vucetic and Mortezaie [29]. Such variation in resilient modulus may be attributed to the coupling effects of EPWP and the adjustment of microstructure. As shown in Fig. 1b, significant EPWP accumulates during the first few cycles, resulting in notable stiffness degradation. After that, EPWP accumulates at a much lower rate, while the sample adjusts the microstructure as loading cycles continue. This may lead to an increase in the stiffness. Another possible reason for the stiffness increase may be attributed to the small strain behaviour of clay under undrained cyclic loading condition as claimed by Qian et al. [19]. Since the sample is subjected to consecutive cyclic loading, the resilient modulus changes continuously and steadily. Figure 8b–d shows the variation of resilient moduli of the samples UD2, DD1 and AD7, respectively. For the samples UD2 and DD1, even though the stiffnesses decrease in the first few cycles after including stress disturbance, they finally increase to the values at the end of the first cyclic loading stage. For the sample AD7, however, the final resilient modulus is smaller than that at the end of the first bundle of 5000 cycles.

Figure 9a reveals the dependence of resilient modulus on the stress states (q/p'^b) at the beginning of the second bundle of loading cycles (after introducing stress disturbance). In the figure, Mr_{5000} and $Mr_{10,000}$ refer to the resilient moduli at the end of the first and the second cyclic loading stages, respectively, and the ratio of $Mr_{10,000}$ to Mr_{5000} reflects the variation of the stiffness during the second cyclic loading stage.

As can be seen, the variation of stiffness can be grouped into two clusters depending on whether q/p'^b is greater or less than 0.27 which is the stress state in the samples at the end of the first bundle of 5000 cycles. For the samples with q/p'^b less than or equal to 0.27, as illustrated in Table 2, the static deviatoric stress decreases or keeps unchanged after including stress disturbance. The resilient moduli at the end of cyclic loading are almost the same with those at end of the first bundle of 5000 cycles. This indicates that including stress disturbance has limited effects on the stiffness if the static deviatoric stress in soil is anticipated to decrease or remain unchanged. In contrast, if static deviatoric stress increases after the stress disturbance, the resilient modulus decreases as q/p'^b value increases. For example, for the sample AD3 with q/p'^b of 0.31, $Mr_{10,000}$ is about 95% of Mr_{5000}. When q/p'^b increases to 0.47 in the sample AD13, $Mr_{10,000}$ is about 34% of Mr_{5000}.

The dependence of resilient modulus on effective mean stress ($p'_{10,000}$) at the end of the second loading stage is illustrated in Fig. 9b where $Mr_{10,000}$ increases with the increase of $p'_{10,000}$, as expected. The variation of stiffness during the second loading stage can be explained with the change of EPWP accumulation as indicated in Fig. 9a and the variation of effective mean stress as shown Fig. 9b. For the samples with q/p'^b less than or equal to 0.27, as shown in Fig. 9a, very limited EPWPs are accumulated. This leads to limited reduction in effective mean stress in the samples during the second cyclic loading stage and therefore limited change in resilient modulus has been observed. However, for those samples with q/p'^b greater than 0.27, since additional static deviatoric stress was induced, notable EPWP accumulated during the second cyclic loading stage, and the greater the q/p'^b value, the greater the EPWP accumulation and the less the effective mean stress at the end of cyclic loading. Therefore, greater stiffness degradation is expected in samples with greater q/p'^b value after stress disturbance.

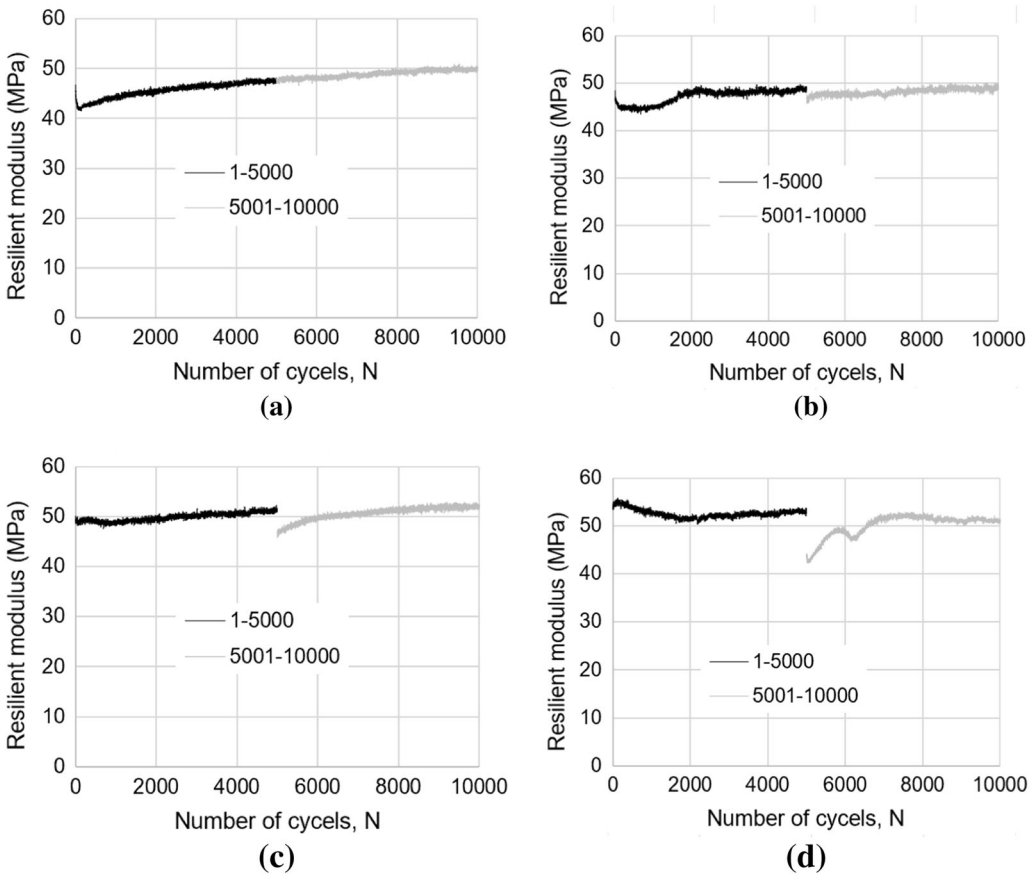

Fig. 8 The variation of resilient modulus of the samples, **a**: UD1, **b** UD2, **c** DD1, **d** AD7

4 Excavation caused hotspots for cyclic loading-induced settlement of existing tunnels

As discussed earlier, the cyclic deformation behaviour of clay in the subsequent bundle of loading cycles is governed by the stress disturbance-induced static deviatoric stress, and the construction of a pit or tunnel will change stress states in soil at different locations along different stress paths [10, 27]. This means that the effects of such construction activities on traffic loading-induced settlement of existing tunnels varies from locations, if those existing structures are within the influenced zones. Based on the additional stress caused by nearby construction activities and the strain accumulation under different stress disturbance schemes, the hotspots for traffic loading-induced settlement of existing structures can be classified. This section discusses the possible impact of construction activities, such as the construction of a pit or tunnel, on traffic loading-induced settlement in existing tunnels using two examples.

Scenario 1: the excavation of a new pit adjacent to an existing tunnel. As shown in Fig. 10a, a new pit is to be excavated next to, diagonally above or directly above an existing tunnel. For the three cases, the excavation will have different effects on the long-term settlement of the tunnel if traffic loading in the tunnel is of concern to its long-term settlement. This is because the additional stress due to excavating the pit varies with locations as revealed in Fig. 10b, as investigated by many researchers [8, 11, 17, 37, 38]. For example, within zone 1, as suggested by Huang et al. [10], the deviatoric stress in the soil would increase, and mean principal stress would decrease. If the existing tunnel is in this zone, then the traffic loading in the tunnel could potentially cause more settlement due to the increase of deviatoric stress in the soil. If the existing tunnel is in zone 3, where the deviatoric stress decreases after the excavation, then the effect of traffic loading-induced settlement of the tunnel could be ignored, as the decrease of deviatoric stress would cause little additional deformation under subsequent cyclic loading as discussed above. For zone 2, due to complexity of the variation in deviatoric stress as suggested by Huang et al. [10], it is harder to tell whether the excavation will affect the traffic loading-induced long-term settlement of the existing tunnel. Therefore, if the existing tunnel is within zone 2, then

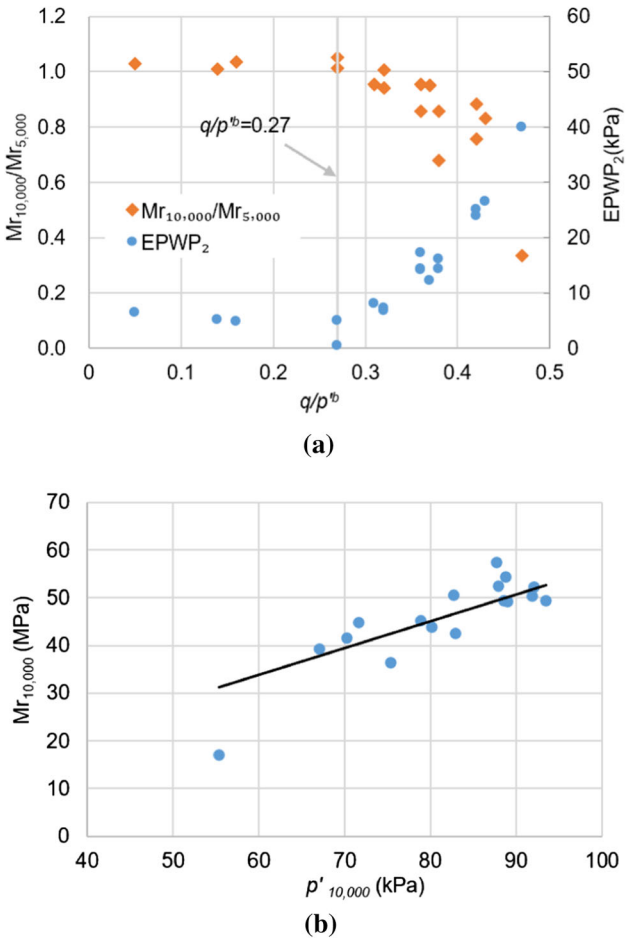

Fig. 9 **a** The variations of resilient modulus and excess pore water pressure ($EPWP_2$) accumulated during the second bundle of loading cycles and **b** the dependence of resilient modulus on the effective mean stress ($p'_{10,000}$) at the end of cyclic loading (Mr_{5000}: the resilient modulus after the first cyclic loading stage; $Mr_{10,000}$: the resilient modulus after the second cyclic loading stage)

traffic loading-induced tunnel settlement should be considered on a case-by-case basis.

Scenario 2: the excavation of a new tunnel adjacent to an existing tunnel. Typical locations of the new tunnel in relation to the existing tunnel are shown in Fig. 11. In the figure, three typical locations are considered. To analyse the effect of tunnelling on the stress disturbance in ground, Verruijt' solution [27] is used to obtain the variation of lateral and vertical stresses around the new tunnel as revealed in Fig. 12. In the figure, the tunnel is buried at the depth of 2D where D is the outside diameter of the tunnel. A uniform radial displacement of $0.01D$ is applied at the boundary of the circular cavity, leading to a ground loss of about 4%. Poisson's ratio of the soil is assumed to be 0.33. The marks of "−" and " + "in the figure suggest stress decreasing and increasing, respectively.

Considering that the major principal stress in the soil is on vertical direction, using the stress variation described in Fig. 12, we can get:

(1) if the proposed tunnel is to be excavated directly above or below the existing tunnel as illustrated in Fig. 11a, the excavation will cause the reduction of vertical stress and increase of lateral stress in the soil. This will result in the reduction of deviatoric stress. In this case, the new tunnel would have limited effect on the traffic loading-induced settlement of the existing tunnel.

(2) If the proposed tunnel is to be excavated next to the existing tunnel as revealed in Fig. 11b, the excavation is likely to cause the reduction of lateral stress and increase of vertical stress in the soil around the existing tunnel, depending on the distance between the two tunnels. This may increase the deviatoric stress in the soil around the existing tunnel. In this case, the new tunnel would possibly induce additional traffic loading-induced settlement to the existing tunnel. In addition, as shown in Fig. 12, the closer the new tunnel to the existing tunnel, the greater the reduction in lateral stress, resulting in greater additional static deviatoric stress, therefore the greater the impact on the existing tunnel in terms of traffic loading-induced settlement as illustrated in Fig. 7.

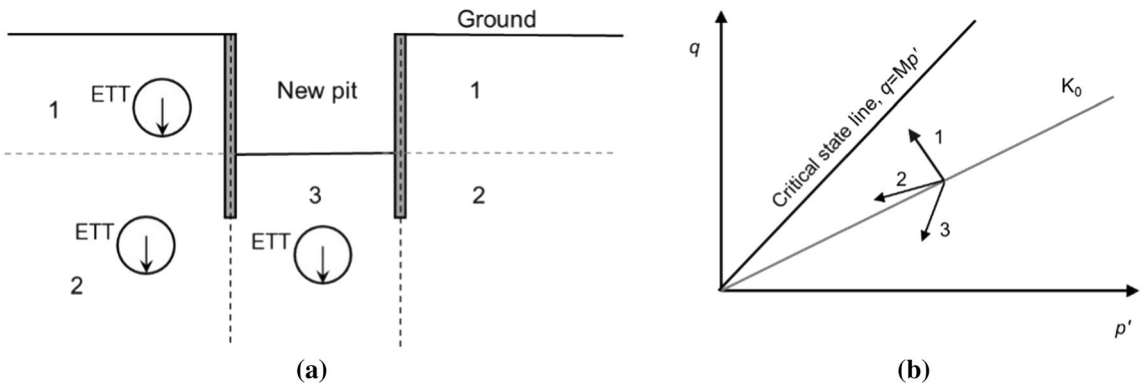

Fig. 10 **a** The relative location of the existing traffic tunnel (ETT) to the new excavation and **b** the stress paths in different locations around the pit (after Huang et al. [10])

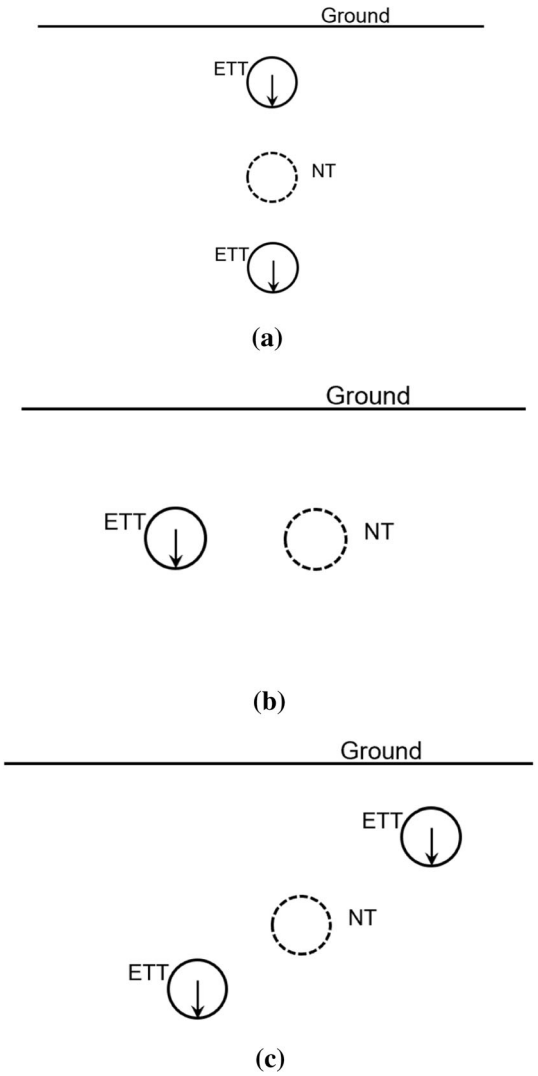

Fig. 11 The relation between the existing traffic tunnel (ETT) and possible location of a new tunnel (NT), **a** NT directly above or below ETT, **b** NT next to ETT and **c** NT on the top (or bottom) right (or left) of ETT

(3) If the proposed tunnel is on the top (or bottom) right (or left) of the existing tunnel as shown in Fig. 11c, then the effect needs to be considered on a case-by-case basis, as the deviatoric stress in the soil around the existing tunnel could increase or decrease depending on the location of the new tunnel.

5 Summary and conclusions

To evaluate the effects of interspersing stress disturbance between loading cycles on the long-term deformation behaviour of soft clay, a series of undrained cyclic triaxial tests were performed on a normally consolidated kaolin clay. The stress disturbance was simulated by changing the

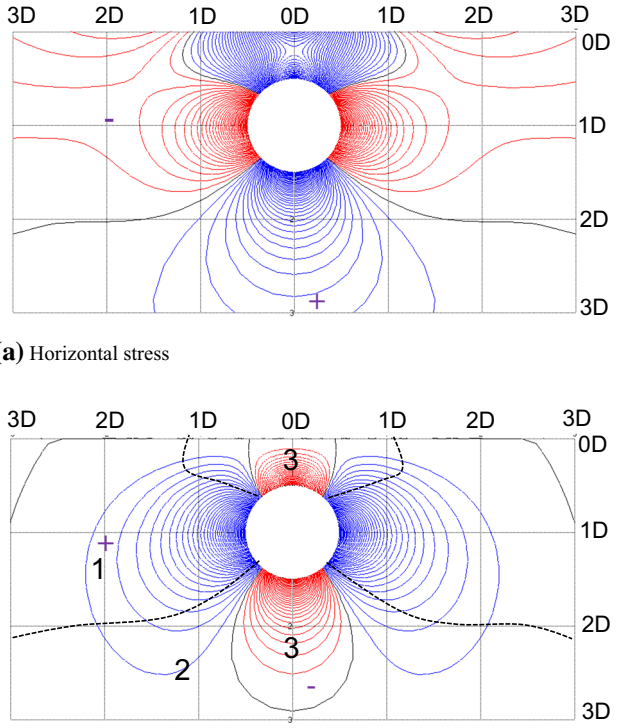

Fig. 12 Tunnelling-induced additional stress obtained using Verruijt's solution [27]. In the figure, the black lines indicate the planes with no change in stress; the bule lines are contours of stress increment; and the red lines are contours of stress reduction. The intervals are 0.001G, where G is modulus of rigidity of the soil

lateral and vertical stresses between loading cycles along different stress paths. The axial strain and excess pore water pressure accumulations and stiffness variation were presented and discussed under different stress disturbance schemes. From the limited number of tests, it was found that:

(1) The axial strain and excess pore water pressure accumulations in the subsequent bundle of loading cycles are governed by the stress disturbance-induced static deviatoric stress. If the stress disturbance leads no change in static deviatoric stress, axial strain accumulation in the sample increases slightly in the early few cycles after stress disturbance and then roughly follows the tendency of that prior to the stress disturbance. For the samples subjected to the reduction of deviatoric stress, axial strain accumulation increases slightly in the early few cycles after stress disturbance and then eliminates afterwards, regardless of the stress disturbance schemes. In contrast, for samples where static deviatoric stress increases, the rate of strain accumulation will re-increase after stress disturbance and the greater the additional static deviatoric stress, the greater the increment. Such phenomena suggest that the stress disturbance caused by nearby construction activities should be

considered in analysing the long-term settlement of existing structures subjected to cyclic loading if the proposed structure is anticipated to increase the static deviatoric stress in the soil supporting the existing structures.

(2) After increasing the static deviatoric stress, the axial strain accumulation in the sample would increase exponentially with the static deviatoric stress ratio and is independent to the schemes of stress disturbance.

(3) If the induced stress disturbance would increase the static deviatoric stress ratio in the samples, notable stiffness degradation can be found during the subsequent loading cycles, and the greater the static deviatoric stress ratio, the greater the stiffness degradation. If stress disturbance induces no change or increment of static deviatoric stress ratio in the samples, then the stress disturbance would have limited effects on the stiffness.

(4) Preliminary analysis shows that if the excavation of a pit or a tunnel is next to the existing tunnel, the excavation is likely to have more impact on traffic loading-induced settlement in the existing tunnel comparing to excavations above or below the existing tunnel.

It is to note that the tests in this study were carried out under an undrained condition. To simulate the long-term drainage process during construction and cyclic loading durations, a more complicated drainage condition should be considered in the tests.

Acknowledgements The project is funded by the Zhejiang Provincial Institute of Communications Planning, Design & Research and the Systematic Project of Guangxi Key Laboratory of Disaster Prevention and Structural Safety (2019ZDX021). The first author received Ph.D. scholarship from the University of New South Wales. The first author would like to thank Dr Zonghui Liu, Mr Tenglong Liang and Mr Xingyu Luo from the College of Civil engineering and Architecture at Guangxi University for their help during the tests.

References

1. Alam MJI, Gnanendran CT, Lo SR (2017) Modelling the settlement behaviour of a strip footing on sloping sandy fill under cyclic loading conditions. Comp Geotech 86:181–192
2. Brown SF (1996) Soil mechanics in pavement engineering. Géotechnique 46(3):384–426. https://doi.org/10.1680/geot.1996.46.3.383
3. Chai JC, Miura N (2002) Traffic-load-induced permanent deformation of road on soft subsoil. J Geotech Geoenviron Eng 128(11):907–916. https://doi.org/10.1061/(Asce)1090-0241(2002)128:11(907)
4. Chen C, Zhou ZM, Kong LW, Zhang XW, Yin S (2018) Undrained dynamic behaviour of peaty organic soil under long-term cyclic loading, Part I: experimental investigation. Soil Dyn Earthq Eng 107:279–291. https://doi.org/10.1016/j.soildyn.2018.01.012
5. Cheng H, Chen R, Wu H, Meng F (2020) A simplified method for estimating the longitudinal and circumferential behaviors of the shield-driven tunnel adjacent to a braced excavation. Comp Geotech 123:103595. https://doi.org/10.1016/j.compgeo.2020.103595
6. Di H, Zhou S, Xiao J, Gong Q, Luo Z (2016) Investigation of the long-term settlement of a cut-and-cover metro tunnel in a soft deposit. Eng Geol 204:33–40. https://doi.org/10.1016/j.enggeo.2016.01.016
7. Do NA, Dias D, Oreste P, Djeran-Maigre I (2014) Three-dimensional numerical simulation for mechanized tunnelling in soft ground: the influence of the joint pattern. Acta Geotech 9(4):673–694. https://doi.org/10.1007/s11440-013-0279-7
8. Dolealova M (2001) Tunnel complex unloaded by a deep excavation. Comp Geotech 28(6–7):469–493. https://doi.org/10.1016/S0266-352X(01)00005-2
9. Ge SP, Yao XJ, Ye B, Pu ST, Liu XZ (2016) Analysis of long-term settlement of soft clay under train vibration. Chin J Rock Mech Eng 35(11):2359–2368
10. Huang H, Huang M, Ding JS (2018) Calculation of tangent modulus of soils under different stress paths. Math Probl Eng 2018:1916761. https://doi.org/10.1155/2018/191676
11. Huang M, Liu XR, Zhang NY, Shen QW (2017) Calculation of foundation pit deformation caused by deep excavation considering influence of loading and unloading. J Cent South Univ 24(9):2164–2171. https://doi.org/10.1007/s11771-017-3625-3
12. Hyde AFL, Brown SF (1976) The plastic deformation of a silty clay under creep and repeated loading. Géotechnique 26(1):173–184. https://doi.org/10.1680/geot.1976.26.1.173
13. Hyde AFL, Yasuhara K, Hirao K (1993) Stability criteria for marine clay under one-way cyclic loading. J Geotech Eng ASCE 119(11):1771–1789
14. Hyodo M, Yamamoto Y, Sugiyama M (1994) Undrained cyclic shear behaviour of normally consolidated clay subjected to initial static shear stress. Soils Found 34(4):1–11. https://doi.org/10.3208/sandf1972.34.4_
15. Jamali H, Tolooiyan A, Dehghani M, Asakereh A, Kalantari B (2018) Long-term dynamic behaviour of Coode Island Silt (CIS) containing different sand content. Appl Ocean Res 73:59–69. https://doi.org/10.1016/j.apor.2018.02.002
16. Liu ZY, Xue JF, Yaghoubi M (2021) The effects of unloading on undrained deformation of a kaolin clay under cyclic loading. Soil Dyn Earthq Eng 140:106434. https://doi.org/10.1016/j.soildyn.2020.106434
17. Ng CWW (1999) Stress paths in relation to deep excavations. J Geotech Geoenviron Eng 125(5):357–363. https://doi.org/10.1061/(asce)1090-0241(1999)125:5(357)
18. Ou X, Zhang X, Fu J, Zhang G, Zhou X (2019) Cause investigation of large deformation of a deep excavation support system subjected to unsymmetrical surface loading. Eng Fail Anal 107:104202. https://doi.org/10.1016/j.tust.2020.103380
19. Qian J, Du Z, Lu X, Gu X, Huang M (2019) Effects of principal stress rotation on stress-strain behaviors of saturated clay under traffic-load-induced stress path. Soils Found 59(1):41–55. https://doi.org/10.1016/j.sandf.2018.08.014
20. Qian J, Du Z, Yin Z (2018) Cyclic degradation and non-coaxiality of soft clay subjected to pure rotation of principal stress directions. Acta Geotech 13(4):943–959
21. Qian JG, Li SY, Zhang JL, Jiang JH, Wang QY (2019) Effects of OCR on monotonic and cyclic behavior of reconstituted Shanghai silty clay. Soil Dyn Earthq Eng 118:111–119. https://doi.org/10.1016/j.soildyn.2018.12.010
22. Qian J, Wang Q, Jiang J, Cai Y, Huang M (2018) Centrifuge modeling of a saturated clay ground under cyclic loading. Int J Geomech 18(6):04018041. https://doi.org/10.1061/(ASCE)GM.1943-5622.0001166
23. Qian JG, Wang YG, Yin ZY, Huang MS (2016) Experimental identification of plastic shakedown behavior of saturated clay

subjected to traffic loading with principal stress rotation. Eng Geol 214:29–42. https://doi.org/10.1016/j.enggeo.2016.09.012
24. Ren XW, Tang YQ, Li J, Yang Q (2012) A prediction method using grey model for cumulative plastic deformation under cyclic loads. Nat Hazards 64:441–457. https://doi.org/10.1007/s11069-012-0248-8
25. Shen SL, Wu HN, Cui YJ, Yin ZY (2014) Long-term settlement behaviour of metro tunnels in the soft deposits of Shanghai. Tunn Undergr Space Technol 40:309–323. https://doi.org/10.1016/j.tust.2013.10.013
26. Strack OE (2002) Analytic solutions of elastic tunneling problems. Ph.D. thesis, Delft University of Technology
27. Verruijt A (1997) A complex variable solution for a deforming circular tunnel in an elastic half-elastic plane. Int J Numer Methods Geomech 21:77–89
28. Verruijt A, Booker JR (1998) Surface settlements due to deformation of a tunnel in an elastic half plane. Géotechnique 46(5):753–756. https://doi.org/10.1680/geot.1998.48.5.709
29. Vucetic M, Mortezaie A (2015) Cyclic secant shear modulus versus pore water pressure in sands at small cyclic strains. Soil Dyn Earthq Eng 70:60–72
30. Wang Y, Gao Y, Li B, Guo L, Cai Y, Mahfouz AH (2019) Influence of initial state and intermediate principal stress on undrained behavior of soft clay during pure principal stress rotation. Acta Geotech 14(5):1379–1401. https://doi.org/10.1007/s11440-018-0735-5
31. Wang Y, Wan Y, Liu M, Guo C, Zeng C, Wu D (2020) Undrained multi-dimensional deformation behavior and degradation of natural soft marine clay from HCA experiments. Soils Found 60(1):103–114. https://doi.org/10.1016/j.sandf.2020.01.002
32. Wichtmann T, Andersen KH, Sjursen MA, Berre T (2013) Cyclic behaviour of high-quality undisturbed block samples of Onsøy clay. Can Geotech J 50(4):400–412. https://doi.org/10.1139/cgj-2011-0390
33. Wu HN, Shen SL, Chai JC, Zhang DM, Xu YS (2015) Evaluation of train-load-induced settlement in metro tunnels. Proc Inst Civ Eng Geotech Eng 168(5):396–406. https://doi.org/10.1680/geng.13.00159.
34. Yang JQ, Cui ZD (2020). Influences of train speed on permanent deformation of saturated soft soil under partial drainage conditions. Soil Dyn Earthq Eng 133:106120. https://doi.org/10.1016/j.soildyn.2020.106120
35. Yang Q, Tang YQ, Yuan B, Zhou J (2019) Cyclic stress-strain behaviour of soft clay under traffic loading through hollow cylinder apparatus: effect of loading frequency. Road Mater Pavement Des 20(5):1026–1058. https://doi.org/10.1080/14680629.2018.1428219
36. Zhang Z, Huang M (2014) Geotechnical influence on existing subway tunnels induced by multiline tunneling in Shanghai soft soil. Comp Geotech 5:121–132. https://doi.org/10.1016/j.compgeo.2013.11.008
37. Zhang XM, Ou XF, Yang JS, Fu JY (2017) Deformation response of an existing tunnel to upper excavation of foundation pit and associated dewatering. Int J Geomech 17(4):04016112. https://doi.org/10.1061/(ASCE)GM.1943-5622.0000814
38. Zhang Z, Zhang M, Zhao Q (2015) A simplified analysis for deformation behavior of buried pipelines considering disturbance effects of underground excavation in soft clays. Arab J Geosci 8(10):7771–7785. https://doi.org/10.1007/s12517-014-1773-4